Scholar Publishing Group
International Journal of Multimedia Computing
https://doi.org/10.38007/IJMC.2023.040105
ISSN 2789-7168 Vol. 4, Issue 1: 69-85

# *An Efficient Algorithm for Multi-dimensional and Multi-point Random Seismic Response Analysis of Spatial Grid Structure based on Computer*

**Xiaoyong Zhang***

*Unicom (Heilongjiang) Industrial Internet Co.,Ltd., Heilongjiang, China*

*zhangxy922@chinaunicom.cn*

**corresponding author*

***Keywords:*** Virtual Excitation Method, Seismic Intensity Determination, Seismic Response Analysis, Multi-dimensional and Multi-point

***Abstract:*** At present, the power spectrum method in the field of random vibration analysis, that is, to calculate the power spectrum of various responses from the given excitation power spectrum, has developed into a mature method. However, this method has not been widely used in engineering design in the past. The purpose of this paper is to study the efficient algorithm of multi-dimensional and multi-point random seismic response analysis of spatial grid structure. Firstly, the paper introduces the quick assessment of earthquake personnel loss from the aspects of the factors affecting the magnitude of earthquake disaster and the assessment process of earthquake personnel loss. Then, it further discusses the theoretical formula of multi-dimensional virtual excitation method, further extends the "virtual excitation method" to the multi-dimensional multi-point non-stationary random earthquake response analysis of spatial grid structure, gives the peak response estimation method, and discusses the multi-dimensional ground, the random model of vibration and the selection of parameters, the random seismic response of latticed shell structure is analyzed by special computer program. The experimental results show that the non-stationary random seismic response of the latticed shell is slightly smaller than that of the stationary random seismic response, with a ratio of about 0.9. The laws of the steady and non-stationary random vibration response of the latticed shell members are similar.

## 1. Introduction

With the continuous development of the times, the continuous improvement of social, economic

and cultural level, and the progress of science and technology, how to effectively use the existing data and data, and apply new methods to improve the ability of the government and the earthquake department to respond quickly to emergencies and resist risks, and provide convenient and quick emergency rescue and related information for the masses is particularly important [1-3]. Earthquake disaster pre assessment software is a software system that integrates multiple disciplines, such as computer, geographic information system, global positioning system, monitoring system, earthquake disaster pre assessment system, statistical system, etc., integrates multiple data through network, communication and other channels, and provides earthquake emergency services and earthquake disaster pre assessment [4-6]. The earthquake disaster pre assessment software can effectively simulate the geological disaster, building collapse, lifeline engineering damage, casualties, economic loss and other disasters after the earthquake. According to the simulated disaster data, the pre disaster preparation work can be done, so that the disaster prevention and mitigation can be implemented, and provide more effective technical support for the post disaster leadership and organization of earthquake relief work [7-9]. Earthquake is a kind of emergency. Earthquake disaster often has the characteristics of strong emergency, high pressure, wide impact, great social impact, long duration, some quasi periodicity and so on. Earthquake disasters often cause serious casualties and economic losses, and can cause secondary disasters such as sand liquefaction, collapse, landslide, debris flow, avalanche and tsunami [10-12]. The earthquake will cause serious casualties, the key reason is that the occurrence of the earthquake will cause serious housing damage [13-15]. In order to reduce the damage caused by the earthquake and make the building structure resist the possible earthquake within the service life, the earthquake resistance ability of the structure should be enhanced as much as possible. The large-span grid structure is a spatial structure system, showing obvious spatial stress and deformation characteristics [16]. Therefore, the combined action of horizontal and vertical earthquake should be considered in the seismic response analysis of spatial grid structure. It can be seen that the analysis of structural seismic response is of great significance [17].

J. An studied the seismic response characteristics under strong horizontal ground motion, and compared with the seismic response characteristics of single-layer rectangular / circular tunnel. The results show that the interaction effect of the two-layer tunnel increases the peak value of the relative horizontal displacement and vibration acceleration of the upper and lower tunnels, and decreases with the increase of the intersection angle. The seismic stress of the top rectangular tunnel increases, while that of the bottom circular tunnel decreases. The interaction effect of cross metro tunnel is closely related to the cross shape of bedrock and the characteristics of input seismic wave. The weak parts of the tunnel structure are the rectangular top of the top layer, the connection between the layer and the side wall, the top and bottom of the column (middle column), the arch shoulder and the circular top of the bottom layer. The seismic deformation modes of rectangular and circular tunnels are similar to the monotonic growth of sinusoidal and inverted S-shaped curves, respectively. The deformation of site soil is mainly shear deformation. When the earthquake occurs, the contact surface between soil and structure is weak [18]. Christelle Salameh conducted a risk and vulnerability assessment of the dynamic parameters of buildings in Beirut (Lebanon) based on the environmental vibration method. Lebanon is facing a high seismic risk due to its major faults, high seismic risk due to intensive urbanization, and lack of implementation of seismic design codes. In this study, 330 reinforced concrete buildings were recorded for environmental vibration, periodic parameters were extracted and analyzed statistically to determine the correlation with physical building parameters (height, horizontal size, age) and site characteristics (rock site or soft site). The results show that: (1) building height or number of floors (n) is the main statistical robust parameter for estimating fundamental wave period T; (2) the correlation between T and N is linear and related to the site: for rock site $t \approx n / 23$, for soft site $n / 18$; (3) the measured damping is inversely

proportional to the period: the higher the building, the lower the damping; (4) there is an obvious overestimation in the current building code cycle. However, some of the significant differences from the building code recommendations may be due to very low load levels [19]. In order to study the seismic performance of the geogrid reinforced rigid retaining wall with saturated backfill, Liyan Wang established a large-scale shaking table test model of the geogrid reinforced rigid retaining wall and the unreinforced earth retaining wall in a large layered shear vessel. The Froude constant in the dimensional analysis theory determines the geometric similarity law of the test wall, which is expressed by the shear velocity of the soil. The similarity ratio of other variables is derived from the geometric similarity ratio. The shear wave velocity of the model site was measured by the seismic dilatometer. Considering the influence of ground motion, the seismic response, wall acceleration, wall lateral displacement, seismic settlement of backfill sand surface and excess pore water pressure in the strain of backfill sand and geogrid are studied. The results show that the far-field seismic wave has more influence on the seismic performance of the reinforced earth retaining wall than the near-field seismic wave, and the geogrid can still effectively improve the seismic deformation capacity of the saturated earth retaining wall. Geogrid can reduce the development of excess pore water pressure and accelerate the dissipation of excess pore water pressure. The geogrid in the middle layer of the reinforced soil plays an important role in the seismic stability of the retaining wall. The root of the geogrid connected with the wall is the key part of the seismic design of the rigid retaining wall reinforced by geogrid. The seismic design of geogrid reinforced rigid retaining wall must consider the far-field or mid far-field seismic wave [20].

In this paper, the “virtual excitation method” is further extended and applied to the multi-dimensional and multi-point non-stationary random seismic response analysis of spatial grid structure. The theoretical formula of the multi-dimensional virtual excitation random vibration analysis method is derived, the peak response estimation method is given, and the random model and parameter selection of multi-dimensional seismic vibration are discussed. The random earthquake of the latticed shell structure is analyzed by the special computer program response. This method automatically includes the correlation terms between the vibration modes and the input seismic components. The calculation is accurate and fast. It is very suitable for the analysis of the random seismic response of the frequency intensive spatial grid structure. It is an efficient random vibration analysis algorithm.

## 2. Proposed Method

### 2.1. Quick Assessment of Earthquake Personnel Loss

(1) Factors affecting the magnitude of earthquake disaster

Earthquake situation factors, natural environment factors and social factors will have a certain impact on the magnitude of earthquake disasters. Among them, earthquake situation factors include earthquake magnitude, earthquake intensity, focal depth, earthquake time, earthquake location and earthquake type, natural environment factors include topography, climate type and geological structure, and social factors mainly include population density, seismic fortification level, economic development degree and regional rescue capacity. Generally, the disaster loss caused by a moderate or strong earthquake is huge, but it can be minimized by strengthening comprehensive defense.

In the case of the same magnitude of earthquake, the degree of damage caused by different regions is also different. This is mainly affected by the following factors.

1) Earthquake magnitude and focal depth

For an earthquake, the larger the energy released by the earthquake, the greater the possible damage or damage, and the magnitude of the earthquake is closely related to the energy released by the earthquake. The energy released by earthquake will be lost and weakened with the propagation

of seismic wave. Therefore, in the case of the same magnitude, the shallower the focal depth, the greater the surface intensity and the higher the degree of damage. Even if the magnitude of an earthquake is not large, it may cause unexpected damage to some shallow earthquakes.

2) Natural environment

Generally speaking, the disaster loss caused by earthquake is more serious than that in plain area because of the influence of soil structure, landform and other natural environment. After the earthquake, the weather conditions such as rainfall and temperature will increase the difficulty of disaster relief, thus affecting the survival rate of buried or seriously injured people.

3) Population density and economic development degree

Earthquake casualties are closely related to the population density within the scope of earthquake influence. The larger the population density, the more casualties caused by the earthquake. And in areas with high degree of economic development and concentrated social wealth, huge earthquake disasters are often caused.

4) Seismic fortification level

One of the most direct reasons for the loss of earthquake personnel and economic loss is the destruction and collapse of houses and other buildings during the earthquake. The seismic performance and quality of buildings directly affect the degree of earthquake disaster. Therefore, it is of great significance to improve the seismic fortification level to reduce the casualties and economic losses caused by the earthquake.

5) Defense against earthquakes

Before a moderate or strong earthquake, whether people have the knowledge of self-help and mutual rescue or not will affect the disaster loss to a great extent. To some extent, the propaganda work of earthquake science popularization can reduce the disaster loss caused by earthquake.

In an earthquake, the damage in different places is usually different. The closer to the source, the more serious the damage. Earthquake intensity is used to measure the degree of earthquake damage. It can also be interpreted as a measure of the intensity of ground vibration during an earthquake. The area closest to the source (epicenter) has the most serious damage and the highest intensity, which is called epicenter intensity. With the distance from the source, the impact of the earthquake is weaker. Therefore, there is only one magnitude of an earthquake, but there are many earthquake intensities. According to the influence of earthquake on the ground, the earthquake area can be divided into several areas with different intensity. Seismic intensity is not only related to magnitude and epicenter distance, but also to focal depth, soil, geological structure and characteristics of engineering buildings.

The attenuation law of seismic intensity is used to describe the relationship between the intensity and the change of epicentral distance. For different types of earthquakes, at present, the main source models are circle models. In the circular model, the source is regarded as a point. If the propagation medium is isotropic, the total energy of the earthquake will be released uniformly from the point to the surrounding. Therefore, the earthquake intensity of each point on the surface with the same epicenter distance is the same, and the isoseismal line of the circular model is circular distribution. Ellipse model is the most widely used source model at present. In ellipse model, the source is still regarded as a point, but the attenuation laws of long axis and short axis need to be considered. The shape of isoseismal line is determined by the attenuation laws of long axis and short axis. For the fault fracture model, the source is linear distribution, and the total energy of the earthquake is uniformly released from the linear source to the surrounding area. Therefore, the intensity of each point on the surface is only related to the shortest distance of the line source. Researchers in the field of earthquake at home and abroad have established different attenuation relations on the attenuation law of intensity. At present, the most commonly used intensity attenuation relationship in China is shown in Formula 1.

$$I = A + BM\text{-}C\ln(R + R_0) \quad (1)$$

Among them, a, B and C are regression coefficients, which can be obtained by regression analysis of historical seismic data, and R0 is the near-field saturation factor.

(2) Loss assessment process of seismic personnel

The rapid assessment of earthquake personnel loss can provide scientific reference for the government earthquake emergency department to allocate the rescue force, relief materials and medical materials. The rapid assessment of earthquake casualties is mainly to carry out a preliminary assessment of casualties caused by destructive earthquakes. The assessment process of earthquake casualties is as follows:

1) After the occurrence of an earthquake, obtain the information of earthquake quick report at the first time, select the appropriate regional intensity attenuation relationship to calculate the length axis of each isoseismal line through the relevant data in the quick report information, analyze the rupture direction of the earthquake according to the epicenter position and the layer of fault zone, and finally draw the layer of earthquake influence field according to the length and rupture direction of each isoseismal line to determine the influence range of the earthquake.

2) According to the seismic impact field layer and population data layer, using GIS function, carry out spatial overlay analysis and buffer analysis to determine the population under each intensity (if the population data layer used is not the latest, the final intensity area population should be calculated according to the annual population growth rate).

3) Select the most appropriate casualty assessment model according to the geographical location, earthquake time, economic development and housing construction of the disaster area. The personnel evaluation model can be divided into two types according to whether the damage of buildings is considered or not. A detailed building classification system is needed for the casualty model considering the damage of buildings, and the calculation complexity is also high.

4) Using the acquired seismic data, the earthquake casualties in each intensity area are predicted by the casualty assessment model.

5) Write the casualties after assessment into the space layer, and display the assessment results in a graphical or document way.

## 2.2. Other Evaluation after Earthquake

(1) Assessment of damage degree of facilities

In the assessment of the damage degree of farmland, water conservancy projects, oil and gas pipelines, airports, ports and wharves, and key cultural relics, the specific problems to be considered are more complex. In the work of rapid disaster assessment, we can make a simple disaster assessment according to the seismic intensity area where these facilities are located and the seismic grade of the facilities themselves, and produce the location map of the seismic intensity area where these facilities are located. For facilities located in high-level seismic intensity areas and beyond their own seismic fortification level, priority should be given to the exploration and evaluation of the degree of damage. For example, the damage degree of the reservoir and other facilities should be evaluated to determine whether it will cause secondary disasters such as flood. Farmland close to the mountain may be buried by landslides or mudslides, or damaged by ground fissures or sand liquefaction. When oil and gas pipelines are damaged, secondary disasters such as fire or poisoning may occur. The damage caused in the airport and port terminals will lead to the paralysis of transportation, and there will be a large number of people who need evacuation and emergency resettlement. These assessment work not only needs to collect and sort out a large number of basic information data in advance, but also needs to cooperate with other departments and units to carry out troubleshooting work successively after the earthquake, so as to make clear the loss situation of

earthquake disaster.

(2) Evaluation of the demand for rescue materials after the earthquake

In the assessment of the damage degree of farmland, water conservancy projects, oil and gas pipelines, airports, ports and wharves, and key cultural relics, the specific problems to be considered are more complex. In the work of rapid disaster assessment, we can make a simple disaster assessment according to the seismic intensity area where these facilities are located and the seismic grade of the facilities themselves, and produce the location map of the seismic intensity area where these facilities are located. For facilities located in high-level seismic intensity areas and beyond their own seismic fortification level, priority should be given to the exploration and evaluation of the degree of damage. For example, the damage degree of the reservoir and other facilities should be evaluated to determine whether it will cause secondary disasters such as flood. Farmland close to the mountain may be buried by landslides or mudslides, or damaged by ground fissures or sand liquefaction. When oil and gas pipelines are damaged, secondary disasters such as fire or poisoning may occur. The damage caused in the airport and port terminals will lead to the paralysis of transportation, and there will be a large number of people who need evacuation and emergency resettlement. This assessment work not only needs to collect and sort out a large number of basic information data in advance, but also needs to cooperate with other departments and units to carry out troubleshooting work successively after the earthquake, so as to make clear the loss situation of earthquake disaster.

## 2.3. Theoretical Formula of Multidimensional Virtual Incentive Method

For the spatial grid structure system, assuming that the mass is concentrated on each node, and only the effect of three-dimensional translational seismic component is considered, and the effect of rotational component of ground motion is ignored, the absolute coordinate system relative to the rest of the earth center is selected, and assuming that the damping force is proportional to the relative velocity, the motion equation of the system under the multi-point earthquake excitation can be written as follows:

$$\begin{bmatrix} M_{ss} & 0 \\ 0 & M_{mm} \end{bmatrix} \begin{Bmatrix} \ddot{U}_s + \ddot{U}_r \\ \ddot{U}_m \end{Bmatrix} + \begin{bmatrix} C_{ss} & C_{sm} \\ C_{ms} & C_{mm} \end{bmatrix} \begin{Bmatrix} \dot{U}_r \\ 0 \end{Bmatrix} + \begin{bmatrix} K_{ss} & K_{sm} \\ K_{ms} & K_{mm} \end{bmatrix} \begin{Bmatrix} U_s + U_r \\ U_m \end{Bmatrix} = \begin{Bmatrix} 0 \\ P_m \end{Bmatrix} \tag{2}$$

Where: [MSS], [CSS], [KSS] are the mass, damping and stiffness matrices of free joints; [Mmm], [Cmm], [Kmm] are the mass, damping and stiffness matrices of bearing restrained joints; {Csm} , {Cms} are the coupling damping matrices of free joints and bearing joints; {Ksm}, {Kms} are the coupling stiffness matrices of free joints and bearing joints;{Us}, {Ur} are the quasi-static and quasi dynamic displacement vectors of free joints; {Um} is the quasi-static displacement vector of the bearing node, that is, the forced displacement vector of the ground node; {Pm} is the external load vector acting on the bearing node.

Formula (2) is further simplified to:

$$[M_{ss}][\ddot{U}_r] + [C_{ss}]\{\dot{U}_r\} + [K_{ss}]\{U_r\} = [M_{ss}][K_{ss}]^{-1}[K_{sm}]\{\ddot{U}_m\} \tag{2}$$

$$\{U_s\} = -[K_{ss}]^{-1}[K_{sm}]\{U_m\} \tag{3}$$

Assuming that when t = Tj, the seismic wave reaches the j-th support node (Xj, Yj), then:

$$T_j = (X_j \cos\theta + Y_j \sin\theta)/v \tag{4}$$

Where, ν is the equivalent apparent velocity of seismic wave and θ is the angle between the propagation direction of seismic wave and the x-axis direction of structure.

The acceleration vector of the ground support node can be expressed as:

$$\left\{\ddot{U}_m(t)\right\} = [G(t)]\{\ddot{U}_g(t)\} \tag{5}$$

Where: [G (t)] is the matrix of deterministic time envelope function and $\{\ddot{U}_g(t)\}$ is the vector of stationary stochastic process with time delay.

$$[G(t)] = \begin{bmatrix} G_1(t) & & \\ & O \quad 0 & \\ & G_j(t) & \\ & 0 \quad O & \\ & & G_p(t) \end{bmatrix} \tag{6}$$

$$[G_j(t)] = \begin{bmatrix} g_x(t-T_j) & & 0 \\ & g_y(t-T_j) & \\ 0 & & g_z(t-T_j) \end{bmatrix} \tag{7}$$

$$\{\ddot{U}_g(t)\} = [\ddot{U}_{g1}(t) \Lambda\ \ddot{U}_{gj}(t) \Lambda\ \ddot{U}_{gp}(t)]^T \tag{8}$$

$$\{\ddot{U}_{gj}(t)\} = [\ddot{X}(t-T_j) \quad \ddot{Y}(t-T_j) \quad \ddot{Z}(t-T_j)]^T \tag{9}$$

In practical calculation, it can be assumed that gx(t) =gy(t)=gz(t)=g(t), when t < 0,g(t) = 0.

If the damping matrix satisfies the orthogonal condition, formula (2) can be reduced to Q degrees of freedom by the mode decomposition method. The pseudo dynamic displacement vector is expressed as the combination of the first Q modes

$$\{U_r\}\sum_{j=1}^{q}\{\phi_j\}\mu_j = [\Phi]\{\mu\} \tag{10}$$

By substituting and using the mode orthogonality, the following results are obtained:

$$\{\ddot{\mu}\} + diag[2\zeta_j\omega_j]\{\dot{\mu}\} + diag[\omega_j^2]\{\mu\{ = [\beta[\beta\ddot{U}_m\} \tag{11}$$

$$[\beta] = [\Phi]^T[M_{ss}][K_{ss}]^{-1}[K_{sm}] \tag{12}$$

Where, ζj and ωj are the damping ratio and circular frequency of the j-th mode respectively; the mode matrix satisfies the relation [Φ]T [Mss] [Φ] = [I]. The input power spectral density matrix can be written as:

$$[S\ddot{U}_m\ddot{U}_m] = [G(t)]*[S\ddot{U}_g\ddot{U}_g][G(t)]^T \tag{13}$$

Formula:

$$[S\ddot{U}_g\ \ddot{U}_g(\omega)] = [V]*[S(\omega)][V]^T \tag{14}$$

$$[V] = \begin{bmatrix} [I]_{3e}^{i\omega T_1} \\ [I]_{3e}^{i\omega T_2} \\ M \\ [I]_{3e}^{i\omega T_P} \end{bmatrix};\ [S(\omega)] = \begin{bmatrix} S_{xx}(\omega) & S_{xy}(\omega) & S_{xz}(\omega) \\ S_{yz}(\omega) & S_{yy}(\omega) & S_{yz}(\omega) \\ S_{zx}(\omega) & S_{zy}(\omega) & S_{zz}(\omega) \end{bmatrix};\ [I]_3 = \begin{bmatrix} 1 & 0 \\ & 1 \\ 0 & 1 \end{bmatrix} \tag{15}$$

According to the relevant properties of ground motion, the input power spectrum matrix is Hermitian matrix, so it can be decomposed into:

$$[S(\omega)] = \sum_{j=1}^{r} \alpha_j \{\psi_j\} * \{\psi_j\}^T \tag{16}$$

R is the rank of the excitation power spectrum matrix. For three-dimensional seismic input r = 3, αj and {ψj} are the j-th eigenvalue and eigenvector of the matrix respectively. The following virtual excitation vectors are constructed:

$$\{\ddot{U}_{m_j}(t,\omega)\} = \sqrt{\alpha_j}[G(t)][V]\{\psi_j\}e^{i\omega t} \tag{17}$$

By substituting (12), the pseudo dynamic displacement response of the free node caused by it can be obtained as follows:

$$\{U_{r_j}(t,\omega)\} = \int_0^t [\Phi][h(t-\tau)][\beta]\sqrt{\alpha_j}[G(\tau)][V]\psi_j\}e^{i\omega t}d\tau \tag{18}$$

Where [H (T - τ)] is the impulse response function matrix:

$$\left.\begin{aligned} &[h(t-\tau)] = \mathrm{diag}[h_j(t-\tau)] \\ &h_j(t-\tau) = \frac{1}{\omega_{dj}^{e}}-\zeta_j\omega_j(t-\tau)\sin\omega_{dj}(t-\tau) \\ &\omega_{dj} = \omega_j\sqrt{1-\zeta_j^2} \end{aligned}\right] \tag{19}$$

According to formula (18), the pseudo-static displacement of the free joint caused by the virtual excitation vector is as follows:

$$\begin{aligned} \{U_{s_j}(t,\omega)\} &= -[K_{ss}]^{-1}[K_{sm}]\{U_{m_j}(t,\omega)\} \\ &= -[K_{ss}]^{-1}[K_{sm}]\int_0^t(\int_0^{t'}\sqrt{\alpha_j}[G(t)][V]\{\psi_j\}e^{i\omega t}d\tau)dt' \end{aligned} \tag{20}$$

According to the principle of virtual excitation method, the total displacement power spectrum matrix of nodes can be obtained as follows:

$$[SU_{ss}U_{ss}(t,\omega)] = \sum_{j=1}^{r}\{U_{ss_j}(t,\omega)\}^*\{U_{ss_j}(t,\omega)\}^T \tag{21}$$

$$\{U_{ss_j}(t,\omega)\} = \{U_{s_j}(t,\omega)\} + \{U_{r_j}(t,\omega)\} \tag{22}$$

The internal force power spectrum can also be obtained by the above method:

$$[S_{NN}(t,\omega)] = \sum_{j=1}^{r} \{N_j(t,\omega)\}^* \{N_j(t,\omega)\}^T \tag{23}$$

$$\{N_j(t,\omega)\} = [Z_N]\{U_{ss_j}(t,\omega)\} \tag{24}$$

Where: {Nj (t, ω)} is the internal force caused by the virtual excitation vector; [ZN] is the transformation matrix.

The time-varying variance of the nonstationary response of any member's internal force can be obtained from the elements of the corresponding internal force power spectrum matrix:

$$\sigma_{N_i}^2(t) = \int_{-\infty}^{+\infty} S_{N_iN_i}(t,\omega)d\omega \tag{25}$$

## 2.4. Estimation of Peak Response

The mean value and standard deviation of the maximum response value of a linear structure system under stationary earthquake excitation can be expressed as follows:

$$\overline{y_m} = f\sigma_y; \quad \sigma_{ym} = p\sigma_y \tag{26}$$

$$f = \sqrt{2\ln(\nu_y t_d)} + \frac{0.5772}{\sqrt{2\ln(\nu_y t_d)}}; \; p = \frac{\pi}{\sqrt{6}} \frac{1}{\sqrt{21n(\nu_y t_d)}} \tag{27}$$

Where, F and P are peak factors, σy is the mean square deviation of response, νy is the rate of zero change, and td is the time of earthquake motion.

$$\sigma_y^2 = \int_{-\infty}^{+\infty} S_y(\omega)\,d\omega; \quad \nu_y = \frac{1}{\pi}\sqrt{\frac{\lambda_2}{\lambda_0}}; \quad \lambda_0 = \int_{-\infty}^{+\infty} S_y(\omega)\,d\omega; \quad \lambda_2 = \int_{-\infty}^{+\infty} \omega^2 S_y(\omega)\,d\omega \tag{28}$$

λ0 and λ are the zero order and second order spectral moments of the reaction. In order to make use of the results of the above stationary theory, the non-stationary reaction results can be stabilized.

The time-varying variance can be obtained from the non-stationary time-varying power spectrum

$$\sigma_y^2(t) = \int_{-\infty}^{+\infty} S_y(t,\omega)d\omega \tag{29}$$

The equivalent stationary mean square response $\overline{\sigma_y^2}$ can be obtained by averaging the time-varying variance at the time of earthquake motion. For the zero order and second order spectral moments of power spectrum, the equivalent stationary zero order and second order spectral moments $\overline{\lambda_0}(\overline{\lambda_0} = \overline{\sigma_y^2})$ and $\overline{\lambda_2}$ can also be obtained. The peak response of the structure under the input of unsteady ground motion can be approximately obtained by substituting the stationary $\overline{\sigma_y}$, $\overline{\lambda_0}$ and $\overline{\lambda_2}$ for σy, λ0 and λ2, and then using the formulas (27) and (28).

## 2.5. Multidimensional Random Model and Parameter Selection

The multi-dimensional ground motion model can be obtained on the basis of the single component model considering the cross-correlation between the components. For the single dimension components in the model, this paper selects the strength non-stationary model, that is, using the product of a certain time envelope function and a stationary stochastic process to simulate the non-stationary stochastic process. The time envelope function is expressed as follows:

$$g(t) = \begin{cases} (t/t_1)^2 & 0 \le t < t_1 \\ 1 & t_1 \le t \le t_2 \\ e^{-c(t-t_2)} & t \ge t_2 \end{cases} \tag{30}$$

In the formula, C is the attenuation coefficient; T1 and T2 are the first and last time of the stationary section of the main earthquake respectively.

For the stationary stochastic process model, this paper selects the modified filtered white noise model:

$$S(\omega( = \frac{\omega_g^4 + 4\zeta_g^2\omega_g^2\omega^2}{(\omega_g^2 - \omega^2)^2 + 4\zeta_g^2\omega_g^2\omega^2} \frac{\omega^4}{(\omega_f^2 - \omega^2)^2 + 4\zeta_f^2\omega_f^2\omega^2} S_0 \tag{31}$$

Where, S0 is the spectral intensity factor, ζg and ωg are the damping ratio and predominant frequency of the foundation soil respectively. The combination of the two parameters of ζf and ωf can simulate the change of low-frequency energy of ground motion. Generally, ζf = ζg,ωf = 0.1-0.2ωg can be taken.

On the basis of the single dimension model and considering the cross-correlation among the components, the spectral matrix of the multi-dimensional stable ground motion model can be obtained as follows:

$$[S(\omega S(= \begin{bmatrix} S_{xx}(\omega) & S_{xy}(\omega) & S_{xz}(\omega) \\ S_{yx}(\omega) & S_{yy}(\omega) & S_{yz}(\omega) \\ S_{zx}(\omega) & S_{zy}(\omega) & S_{zz}(\omega) \end{bmatrix} \tag{32}$$

In the above formula, X and Y represent the horizontal component, and Z represents the vertical component. Let's discuss how to take each component in the matrix.

For the two horizontal components, the self-spectrum is taken as the same value, and they are considered to be completely correlated, so that the cross spectrum is the same as the expression of the self-spectral density function:

$$Sxx(\omega) = Syy(\omega) = \frac{\omega_{gH}^4 + 4\zeta_{gH}^2\omega_{gH}^2\omega^2}{(\omega_{gH}^2 - \omega^2)^2 + 4\zeta_{gH}^2\omega_{gH}^2\omega^2} \bullet \frac{\omega^4}{(\omega_{fH}^2 - \omega^2)^2 + 4\zeta_{fH}^2\omega_{fH}^2\omega^2} S_{0H} \tag{33}$$

$$S_{xy}(\omega) = S_{yx}(\omega) = \sqrt{S_{xx}(\omega)_{yy}(\omega)} = S_{xx}(\omega) = S_{yy}(\omega) \tag{34}$$

For the vertical component, it has the same form as the horizontal component, but the model parameters are different.

$$S_{zz}(\omega) = \frac{\omega_{gV}^4 + 4\zeta_{gV}^2\omega_{gV}^2\omega^2}{(\omega_{gV}^2 - \omega^2)^2 + 4\zeta_{gV}^2\omega_{gV}^2\omega^2} \bullet \frac{\omega^4}{(\omega_{fV}^2 - \omega^2)^2 + 4\zeta_{fV}^2\omega_{fV}^2\omega^2} S_{0V} \tag{35}$$

The cross spectrum between horizontal and vertical components shall be taken as follows:

$$S_{xz}(\omega) = S_{yz}(\omega) = S_{zx}(\omega) = S_{zy}(\omega) = 0.6\sqrt{S_{xx}(\omega)S_{zz}(\omega)} = 0.6\sqrt{S_{yy}(\omega)S_{zz}(\omega)} \tag{36}$$

The parameters in the above formulas have the following relations:

$$\omega_{gV} = 1.58\omega_{gH}; \quad \zeta_{gV} = \zeta_{gH}; \quad S_{0V} = 0.281S_{0H} \tag{37}$$

## 3. Experiments

### 3.1. Experimental Data Set

In this paper, the 7.0-magnitude earthquake in city A is selected to analyze the research results of this paper. Firstly, the disaster information of 72 hours after the earthquake is grabbed from the Internet. After the spatial processing and classification of place names, the sensible information, house damage and secondary disaster information are used as data sources to determine the seismic intensity, and the results are divided into spatial interpolation and fitting according to the method of isoseismal correction of intensity in the field of disaster assessment technology, the theoretical isoseismal map of quick assessment of earthquake emergency command system is modified and adjusted. Through the analysis and research of the disaster information from the Internet, 12861 pieces of news data from domestic media and industry earthquake networks, 3392 pieces of disaster information from community forums, 16253 pieces of disaster data in total. First of all, according to the magnitude and epicenter coordinates, a place name database within the epicenter scope is established. There are 72 places in the established place name database, including a province, B Province, C Province, a city, etc. then, 16253 captured data are extracted for place name information extraction and disaster classification processing, including 52 places with disaster, corresponding to 32988 disaster data.

### 3.2. Experimental Setup

In this paper, a program for multi-dimensional and multi-point nonstationary seismic response analysis of long-span grid structures is developed. Figure 1 shows a double-layer cylindrical latticed shell with orthorhombic pyramid. Each node on both longitudinal sides is supported by three-way fixed hinge, and each node on both ends is supported by vertical hinge. The span of latticed shell B = 36m, rise span ratio f / b = 0.3, shell length L = 45m, shell thickness h = 1.5m, grid size a × a = 2.5 × 2.5m, bearing uniform load q = 1.0kn/m2. The seismic fortification intensity is 8 degrees (the design basic seismic acceleration value is 0.2g), and the design earthquake group is the first group, class II site soil. Msgs program is used to optimize the size of the shell members. The parameters of the random model of ground motion can be taken as ωg = 13.96rad/s, ζg = 0.8, and the modified spectral intensity factor S 0 = 3.911cm2/s3; the additional parameters ζf = ζg,ωf = 0.1-0.2ωg are taken as 20 order vibration modes, and the damping ratio is taken as 0.02. The comparison of seismic responses of latticed shell structures under different seismic inputs (multi-dimensional and single-dimensional inputs, multi-point and single-point inputs, etc.) can be obtained.

## 4. Discussion

### 4.1. Comparison of Transverse Top Chord Groups across the Center of Cylindrical Latticed Shell

The comparison of the single dimensional and three-dimensional random responses of the bs10 bars is given respectively.

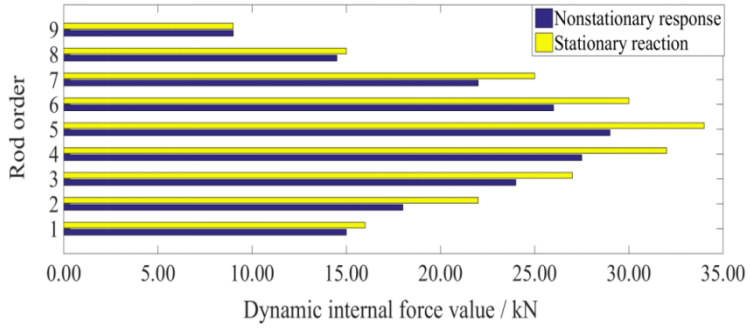


*Figure 1. Comparison of stationary and nonstationary three-dimensional responses of bs10 (Single point)*

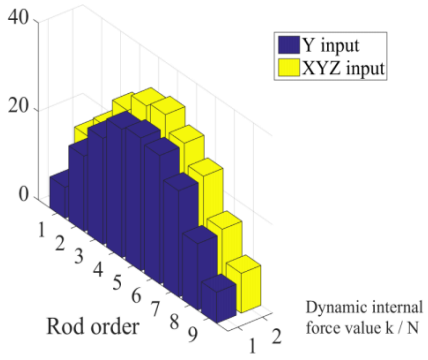


*Figure 2. Comparison of three-dimensional and one-dimensional stationary responses of bs10 (Single point)*

The results show that the non-stationary random seismic response of reticulated shell is slightly smaller than that of the stationary random seismic response under the condition of single or multi-dimensional input, single or multi-point input and so on. The ratio is about 0.9, and the response law of the static and non-stationary random vibration is similar.

### 4.2. Give a Comparison of Responses at Multiple Inputs

The comparison of the single dimensional and three-dimensional random responses of the bs10 bars in the multi-point input (considering the apparent wave velocity of seismic wave V = 2200m / s) is given as shown in Fig. 3 and Fig. 4 respectively.

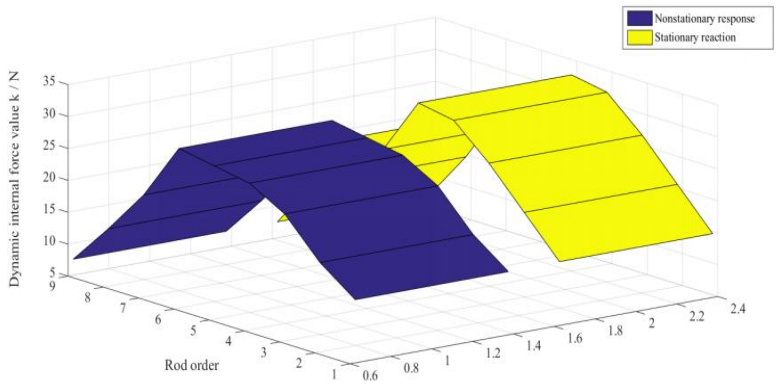


*Figure 3. Comparison of stationary and non-stationary three-dimensional responses of bs10 (Multi-point)*

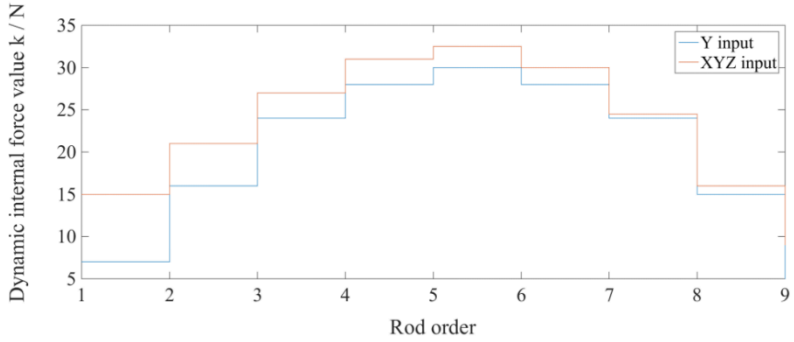


*Figure 4. Comparison of three-dimensional and one-dimensional stationary responses of bs10 (Multi-point)*

Comparison of multi-dimensional and single-dimensional seismic response: the three-dimensional seismic response of members is generally greater than that of single-dimensional seismic response; the distribution rule of three-dimensional and single-dimensional seismic response is generally similar; the dynamic internal force of chords along the upper and lower transverse spans is larger at 1 / 4 span; the dynamic internal force of chords along the longitudinal upper chord is larger at the middle span, while the dynamic internal force of the longitudinal lower chord is larger near the support.

The influence of apparent wave velocity of seismic wave on seismic response: with the change of apparent wave velocity of seismic wave, the dynamic internal force of different members may become larger or smaller, but the change range is not large due to the small plane size of reticulated shell structure.

### 4.3. Determination of Seismic Intensity

After 72 hours data processing, there are 4956 sensitive information, 1460 house damage information, 75 secondary disaster information, 35 points including descriptive words of seismic intensity in 52 Toponymic points, the highest value of the determined intensity is VIII degree, and the points of VI degree, VII degree and VIII degree can be used as the survey data of theoretical Isoseismal map correction. Through the exploratory test on the seismic intensity determination data of 35 toponyms, it is found that the histogram of the data is normal distribution, as shown in Figure

7.2. The maximum intensity area fitted is VIII degree area, which is smaller than the field survey, and the scope of VIII area is larger. A large area of VI degree area appears at the top of the figure, because there is no determination point data in this area, and the result of interpolation has some deviation.

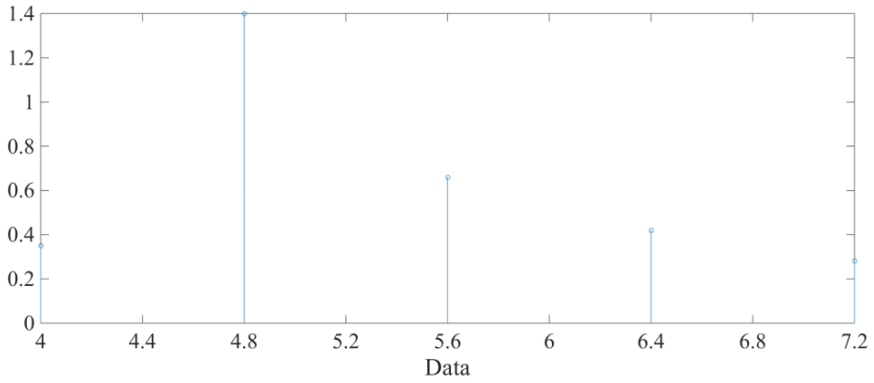


*Figure 5. 72 hours intensity determination data after the earthquake*

Due to the large number of urban disasters near the epicenter and the heavy disaster situation, the revised VI degree area is larger than the actual survey intensity area, and the VII degree area and VIII degree area are closer to the actual survey situation. Because there is no IX degree survey data, the theoretical calculation is taken as the criterion, and the area is smaller than the actual survey area.

Two correction methods are adopted: one is to carry out spatial superposition analysis on theoretical Isoseismal map and place name information, extract theoretical intensity of 103 place name points as interpolation data basis, and carry out spatial interpolation analysis on the basis of VI degree and above place name point data determined in this chapter, and draw the seismic intensity map on the basis of the matching results; the other is to carry out spatial interpolation analysis according to the earthquake site disaster assessment technology. In the method of intensity isoseismal correction, the locations of VI degree and above are taken as survey data, and the theoretical Isoseismal map is modified manually.

Finally, calculate the area of all levels of intensity areas in the seismic intensity map, calculate and compare the area of all levels of intensity areas in the theoretical Isoseismal map of rapid assessment of emergency command system, the intensity map drawn by spatial interpolation fitting combining the intensity points of theoretical calculation and the intensity points determined by network disaster, the intensity map modified manually and the intensity map of field investigation, as shown in Table 1.

*Table 1. Comparison of seismic intensity correction area (unit: km2)*

| Intensity area | Theoretical calculation area | Area corrected by interpolation | Area after manual correction | Field survey area |
|---|---|---|---|---|
| Region VI | 31670 | 31942 | 33510 | 13027 |
| Region VII | 5736 | 7406 | 10431 | 4029 |
| Region VIII | 684 | 2210 | 1546 | 1418 |
| Region of magnitude 9 | 13 | 0 | 0 | 208 |

## 5. Conclusion

In this paper, the "virtual excitation method" is further extended to the analysis of multi-dimensional and multi-point non-stationary random seismic response of spatial grid structure. The theoretical formula of multi-dimensional virtual excitation random vibration analysis method is derived, and the random model and parameter selection of multi-dimensional ground motion are discussed. The random seismic response of latticed shell structure is analyzed by special computer program. This method automatically includes the correlation terms between the vibration modes and the input seismic components. The calculation is accurate and fast. It is very suitable for the analysis of the random seismic response of the frequency intensive spatial grid structure. It is an efficient random vibration analysis algorithm. This method provides an effective basis for studying the seismic performance of spatial grid structure under multi-dimensional seismic action by using stochastic theory.

Taking a mountain earthquake as an example, this paper makes an experimental analysis of the research results. Firstly, 16253 disaster data are collected 72 hours after the earthquake. There are 72 place names in the epicenter, 52 of which contain disaster information. 16253 disaster data are extracted and classified. After processing, there are 32988 disaster information. Among them, there are many disaster data in city a and county B, 4956 sensible information and 1460 house damage information. There are 75 secondary disaster information, including 35 place names with descriptive words of earthquake intensity. The earthquake intensity of 35 place names is determined, and the disaster information of 35 place names is analyzed by spatial interpolation and fitting. At the same time, the theoretical Isoseismal map of rapid evaluation of the earthquake emergency command system is modified and adjusted with the determined earthquake intensity points as survey data.

Based on the study of the case that the ground motion is a stationary random process and a uniform input, this paper further extends the virtual excitation method to the random response analysis of long-span spatial grid structure under the action of multi-dimensional and multi-point non-stationary earthquake, gives the virtual excitation multi-dimensional random vibration analysis method, studies the random model and parameters of multi-dimensional ground motion, and compiles a special computer score analysis of procedures. Finally, the random seismic response of a double-layer cylindrical latticed shell is analyzed, and the response performance under various conditions is compared, and the corresponding conclusions are given.

## Funding

This article is not supported by any foundation.

## Data Availability

Data sharing is not applicable to this article as no new data were created or analysed in this study.

## Conflict of Interest

The author states that this article has no conflict of interest.

## References


[1] Chuhan Z, Yanjie X U, Guanglun W, et al. Non-linear seismic response of arch dams with contraction joint opening and joint reinforcements. Earthquake Engineering & Structural Dynamics. (2015) 29(10): 1547-1566. https://doi.org/10.1002/1096-9845(200010)29:10<1547::AID-EQE979>3.0.CO;2-N

[2] Glenda Abate, Maria Rossella Massimino. Numerical modelling of the seismic response of a tunnel-soil-aboveground building system in Catania (Italy). Bulletin of Earthquake Engineering. (2016) 15(1): 469-491. https://doi.org/10.1007/s10518-016-9973-9

[3] Xiang Y, Luo Y, Guo X. Simplified model and procedure for elasto-plastic seismic response analysis of spatial structure. Journal of Southeast University. (2015) 45(4): 750-755.

[4] Li Zhang, Youjin Su, Ruijie Luo. The Co-seismic Response of Underground Fluid in Yunnan to the Nepal M_S8.1 Earthquake. Earthquake Research in China. (2017) 31(2): 201-212.

[5] Jos é A. Pincheira, Jirsa J O. Seismic response of RC frames retrofitted with steel braces or walls. Journal of Structural Engineering. (2015) 121(8): 1225-1235. https://doi.org/10.1061/(ASCE)0733-9445(1995)121:8(1225)

[6] Kamel Sayed Ahmad Kandil, Ghada N Saudi, B Eltaly. Seismic response of a full-scale wind turbine tower using experimental and numerical modal analysis. International Journal of Advanced Structural Engineering. (2016) 8(4): 337-349. https://doi.org/10.1007/s40091-016-0130-0

[7] Cengizhan Durucan, Murat Dicleli. A P /V P specific inelastic displacement ratio for seismic response estimation of structures. Earthquake Engineering & Structural Dynamics. (2015) 44(7): 1075-1097. https://doi.org/10.1002/eqe.2500

[8] Biao Wei, Peng Wang, Xuhui He. The Impact of the Convex Friction Distribution on the Seismic Response of a Spring-friction Isolation System. Ksce Journal of Civil Engineering. (2017) 22(6): 1-11. https://doi.org/10.1007/s12205-017-0938-6

[9] Lu X, Wang D, Wang S. Investigation of the seismic response of high‐rise buildings supported on tension‐resistant elastomeric isolation bearings. Earthquake Engineering & Structural Dynamics. (2016) 45(13): 2207-2228. https://doi.org/10.1002/eqe.2755

[10] Li X J, Hou C L, Pan R, et al. Effect of damping matrix selection on seismic response of nuclear power plant structures. Journal of Vibration & Shock. (2015) 34(1): 110-116. https://doi.org/10.1155/2015/760394

[11] Bougacha S, Tassoulas J L. Seismic Response of Gravity Dams. II: Effects of Sediments. Journal of Engineering Mechanics. (2016) 117(8): 1839-1850. https://doi.org/10.1061/(ASCE)0733-9399(1991)117:8(1839)

[12] Guo J, Fan H. Seismic response properties of steel concentric X-centrically steel braced RC frames. Journal of Central South University. (2015) 46(6): 2299-2308.

[13] Tomoda A, Watanabe T, Tanaka K. Seismic Response of a Two-Degree-of-Freedom System with Friction Based on the Mass Ratio. Lobachevskii Journal of Mathematics. (2017) 38(3): 525-529.

[14] Li Z Y, Jiang L Y, Li Z L. Effect of bearing model on the seismic response of curved continuous girder bridge. Journal of Vibration & Shock. (2015) 34(2): 182-186.

[15] Wancheng Yuan, Xiaowei Qu. Application Analysis of Seismic Isolation Devices on Longitudinal Seismic Response of Floating System Cable-stayed Bridge. Journal of Tongji University. (2015) 43(2): 199-204.

[16] Hu H, Zhou X, Wang J. A wave numerical method for seismic response of tunnels in bedding strata. Chinese Journal of Rock Mechanics & Engineering. (2017) 36(6): 1373-1383.

*[17] Sun Z, Kong L, Guo A. Centrifuge modeling tests on seismic response of lower bedrock deposit slopes before and after reinforced with stabilizing piles. Chinese Journal of Rock Mechanics & Engineering. (2017) 36(6): 1413-1423.*

*[18] An J, Tao L, Li J. Nonlinear seismic response of double-decked intersecting metro tunnel. China Railway Science. (2015) 36(3): 66-72.*

*[19] Christelle Salameh, Bertrand Guillier, Jacques Harb. Seismic response of Beirut (Lebanon) buildings: instrumental results from ambient vibrations. Bulletin of Earthquake Engineering. (2016) 14(10): 1-26. https://doi.org/10.1007/s10518-016-9920-9*

*[20] Wang L, Chen G, Chen S. Experimental study on seismic response of geogrid reinforced rigid retaining walls with saturated backfill sand. Geotextiles & Geomembranes. (2015) 43(1): 35-45. https://doi.org/10.1016/j.geotexmem.2014.11.006*